International Journal of Applied Engineering Research
ISSN 0973-4562 Volume 21, Number 3 (2026) pp. 373-390
Research India Publications
https://www.ripublication.com

Blower-Assisted Vacuum Dust Capture for Capacitor Winding Machines: A CFD-DPM Study

Mohd Faid Yahya*[1], Nahvin Arul Sekaran[1] and Mad Helmi Ab. Majid[2]
[1]Faculty of Electrical Technology and Engineering, Universiti Teknikal Malaysia Melaka (UTeM), 76100 Durian Tunggal, Melaka, Malaysia
[2]Faculty of Computing and Meta-Technology, Universiti Pendidikan Sultan Idris, 35900 Tanjong Malim, Perak, Malaysia
**Correspondence: faid@utem.edu.my*

Abstract

Fine metallic dust released during capacitor winding is easily entrained in the surrounding air and disperses before it reaches conventional vacuum inlets. Such dust contaminates finished components, degrades sensor and inspection reliability, and causes functional capacitors to be rejected at the electrical test stage. This paper investigates a blower-assisted vacuum dust capture mechanism, in which a controlled push jet guides airborne particles towards a suction outlet, as a localised retrofit for winding machines. A simplified three-dimensional model of the winding zone was developed from an industrial site observation, and the airflow was solved in ANSYS Fluent using the steady Reynolds-averaged Navier-Stokes equations with the realizable k-ε turbulence model. Dust transport was predicted with a one-way coupled Discrete Phase Model (DPM) using 277 tracked particle streams of 5 μm aluminium-based dust. Four configurations were compared: no system, vacuum only, blower only and combined blower-vacuum, with blower velocities of 3, 5, 7 and 10 m/s for the combined case. Without any system, and with the blower alone, no particles reached the outlet, giving a capture efficiency of 0%. The vacuum alone captured 75 of 277 particle streams (27%), as suction influence decayed rapidly away from the inlet. All combined blower-vacuum cases transported every tracked particle to the outlet (100%). Among them, 7 m/s gave the best balance of stable airflow and direct particle transport, with terminal drag far below the stability limit, whereas 10 m/s increased turbulence without further benefit. The results show that guiding the airflow, rather than increasing suction alone, can substantially improve local dust capture around winding machines.

Keywords: blower-assisted dust capture; push-pull ventilation; computational fluid dynamics; discrete phase model; realizable k-ε model; winding machine; metallic dust

1. Introduction

Many manufacturing processes generate fine particulate matter through friction, surface contact and mechanical abrasion between moving parts [1], [2]. In winding and roller-based operations, these mechanisms release micro-sized metallic particles that are light enough to become airborne and follow the local air currents rather than settle under gravity [1]. Once airborne, the particles spread beyond the point of generation and deposit on machine elements, product surfaces and inspection equipment. In precision manufacturing, where air cleanliness directly affects product quality, even small quantities of such dust are undesirable [3].

The problem is particularly acute in capacitor production. After the anode and cathode terminals are wound and assembled, each capacitor undergoes an electrical performance test in which 15 V is applied across its terminals. Fine metallic dust deposited on the capacitor surface or the terminal contact areas can disturb this test, so that a correctly functioning capacitor is rejected. Dust that accumulates on rollers, bearings, optical sensors and cameras also increases wear, causes false inspection results and raises the frequency of cleaning and unplanned maintenance. In addition, airborne fine particles raise occupational health concerns for operators working near the machines.

Industrial dust control currently relies mainly on general ventilation, local exhaust ventilation (LEV) and vacuum-based collection. Vacuum inlets placed near rollers and guides are simple and reliable, and they remove settled dust and particles close to the suction opening effectively. However, the velocity field created by a suction opening decays rapidly with distance, so particles released only a short way from the inlet lie outside its effective capture zone. In open or semi-enclosed winding machines, rotating rollers, moving foil and background ventilation create local air currents that carry particles away from the inlet before they can be captured. A site observation at a capacitor manufacturing facility in Malaysia confirmed this behaviour: airborne dust remained visible around the winding zone despite an existing vacuum system.

One way to overcome the short reach of suction is to combine it with a directed supply jet. In push-pull ventilation, a push jet is blown across the contaminant source towards an exhaust hood, which then removes the contaminated air [4]. Field and numerical studies have shown that the push flow can raise capture efficiency markedly compared with exhaust alone [5]. These studies, however, concern large open-surface tanks, foundry casting lines and similar large-scale sources. Little has been reported on applying a compact blower-vacuum pair inside a small machine such as a capacitor winder, where the jet must transport fine particles without disturbing delicate components such as the capacitor terminal.

Computational fluid dynamics (CFD) combined with Lagrangian particle tracking is well suited to evaluating such a concept before a prototype is built [6]. The airflow field can be solved with a Reynolds-averaged turbulence model, and the trajectories of individual particles can then be followed through the predicted flow to identify where they deposit, escape or are captured [6], [7].

This paper therefore investigates a blower-assisted vacuum dust capture mechanism for capacitor winding machines using CFD and the Discrete Phase Model

(DPM). The objectives are: (i) to analyse airflow characteristics and dust transport behaviour in a simplified winding machine environment; (ii) to develop a blower-assisted vacuum configuration that transports dust effectively while keeping the capacitor terminal stable under airflow exposure; and (iii) to evaluate the mechanism by comparing particle transport and capture performance with and without airflow intervention. The main contributions are a like-for-like comparison of no-system, vacuum-only, blower-only and combined configurations under identical conditions, and the identification of an operating blower velocity that balances capture performance against flow stability and terminal loading.

The remainder of the paper is organised as follows. Section 2 reviews dust generation, existing dust control methods and the relevant theory. Section 3 describes the conceptual design, geometry, CFD model and particle tracking setup. Section 4 presents and discusses the airflow, pressure and particle transport results, and Section 5 concludes the paper.

2. Literature Review And Theoretical Background

2.1 Dust Generation in Winding Processes

Winding processes move thin foils, films or wires over several rollers, guides and spools at controlled tension and speed. Repeated surface contact, high rotational speed and tension changes release micro-sized fragments from the material surface and the roller contact points [2]. The resulting dust is typically 3-10 μm in size, metallic and irregular in shape. Its small mass means that aerodynamic drag dominates gravity, so particles settle slowly and are carried by even weak air currents generated by rotating parts or room ventilation [1]. Metallic particles may also carry electrostatic charge, which promotes adhesion to sensors, product surfaces and terminal contact areas. Particles in this size range are also respirable, adding an occupational health dimension to the quality problem [8], [9].

2.2 Existing Dust Control Methods

General ventilation dilutes contaminants by supplying clean air and exhausting room air through ceiling or wall openings. It lowers the average dust concentration in a large space but does not capture dust at the source, and higher ventilation rates can carry particles from one machine zone into another. Local exhaust ventilation places hoods close to the source and is considerably more effective, but its performance depends strongly on hood position and on cross-draughts around the hood. Vacuum-based collection is the most common approach on winding machines and works well for settled dust and particles close to the inlet. Because it produces a unidirectional flow towards a single suction point, particles moving against that flow, for example in the wake of a roller, can escape the capture zone. Table 1 summarises these methods together with the push-pull approach on which the present mechanism is based.

Table 1. Comparison of industrial dust control methods for airborne fine dust

Method	Operating principle	Strengths	Limitation for airborne fine dust
General ventilation	Dilutes dust concentration in the workspace	Improves overall air quality	Does not capture dust at the source
Local exhaust ventilation	Suction hood placed near the source	Effective close to the hood	Sensitive to hood position and cross-draughts
Vacuum-based collection	High-suction removal through inlets near rollers	Reliable for settled and nearby dust	Short reach; dispersing particles escape
Push-pull ventilation	Supply jet pushes contaminant towards an exhaust [4], [5]	Extends the effective capture distance	Jet velocity must be matched to the exhaust and nearby components

Anlimah et al. [4] identified distinct flow regimes in push-pull systems, ranging from dispersion to strong suction, and showed that capture depends on matching the push-jet and pull-flow velocities. Kulmala et al. [5] designed a push-pull system for a foundry casting line with the aid of CFD and measured an increase in average capture efficiency from about 40% without the push jet to about 60% with it. CFD has likewise been used to optimise exhaust hood height and flow rate for oil-mist particles at machine tools [10]. These findings indicate that a correctly sized supply jet can extend the reach of an exhaust. They also show that too strong a jet can spread contaminants instead of delivering them to the outlet, which motivates the velocity study in Section 4.

2.3 Governing Equations and Turbulence Modelling

At the velocities considered here (3-10 m/s) the Mach number is below 0.03, so air is treated as an incompressible Newtonian fluid at constant density and viscosity. The steady Reynolds-averaged continuity and momentum equations are [11]:

$$\nabla \cdot U = 0 \qquad (1)$$

$$\rho(\nabla \cdot U)U = -\nabla \mathrm{P} + \nabla \cdot [(\mu + \mu_t)(\nabla U + \nabla U^T)] + \rho g \qquad (2)$$

where U is the mean velocity vector, P the mean pressure, ρ the air density, μ the dynamic viscosity and μt the turbulent (eddy) viscosity. The flow regime is indicated by the Reynolds number based on the 50 mm blower opening:

$$\mathrm{Re} = \frac{\rho V D_h}{\mu} \qquad (3)$$

With ρ = 1.225 kg/m³ and μ = 1.7894 × 10^{-5} kg/m·s, Re ranges from about 10,300 at 3 m/s to 34,200 at 10 m/s, and is about 17,100 at 5 m/s. The flow is therefore turbulent in every case and requires a turbulence model.

The realizable k-ε model of Ayo and Mohd-Ghazali [7] was adopted. It solves transport equations for the turbulent kinetic energy k and its dissipation rate ε, and evaluates the eddy viscosity as μt = ρCμk²/ε. Unlike the standard k-ε model, Cμ is a variable that depends on the local strain and rotation rates, which keeps the normal Reynolds stresses positive. This gives better predictions of jets, flow separation and recirculation [7], [12], all of which occur where a blower jet meets a suction opening, at a modest computational cost.

2.4 Particle Motion and the Discrete Phase Model

In the DPM, each particle stream is tracked in a Lagrangian frame by integrating its force balance through the converged airflow field [6], [12]:

$$\frac{du_p}{dt} = \frac{18\mu}{\rho_p d_p^2}\frac{C_D Re_p}{24}\left(U - U_p\right) + \frac{g(\rho_p - \rho)}{\rho_p} \qquad (4)$$

where up is the particle velocity, ρp the particle density, dp the particle diameter and Rep = ρdp|up - U|/μ the particle Reynolds number. The drag coefficient CD for spherical particles. The first term is the drag acceleration and the second combines gravity and buoyancy.

How closely a particle follows the air is measured by its relaxation time τp and the Stokes number Stk:

$$\tau_p = \frac{\rho_p d_p^2}{18\mu},\ Stk = \frac{\tau_p U}{D_h} \qquad (5)$$

For a 5 μm particle of density 2700 kg/m³, τp ≈ 2.1 × 10^{-4} s and the terminal settling velocity τpg is only about 2 mm/s. At 7 m/s through the 50 mm opening, Stk ≈ 0.03. Since Stk ≪ 1, the particles follow the air streamlines closely, and their fate is governed by the airflow pattern rather than by inertia or gravity. This is why directing the airflow is an effective way to control where the dust goes.

Because the dust mass loading is very small relative to the air mass, one-way coupling is assumed: the air moves the particles, but the particles do not modify the airflow [6], [12].

3. Methodology

3.1 Research Framework

The study followed five stages. First, the dust problem was identified through a site observation of capacitor winding machines and a review of the literature. Second, dust-prone regions and their airflow behaviour were analysed, and a blower-assisted vacuum concept was developed. Third, a simplified three-dimensional model of the winding zone was built in ANSYS SpaceClaim, and the opening sizes and permissible jet velocity were checked analytically. Fourth, the model was meshed and the airflow was solved in ANSYS Fluent, after which particle trajectories were computed with

the DPM. Finally, velocity, pressure, particle tracks and capture efficiency were compared across seven simulation cases.

3.2 Conceptual Design of the Blower-Assisted Capture Mechanism

The mechanism pairs a blower and a vacuum unit on opposite sides of the dust generation zone, as shown in Figure 1. The two units have distinct roles. The blower is not an extraction device: it supplies a controlled jet that pushes airborne particles away from the terminal at the moment they are released. The vacuum unit performs the actual removal, drawing dust-laden air out of the capture zone towards a filter or collection unit. Together they form a flow corridor between the blower outlet and the vacuum inlet, along which particles are carried instead of dispersing into the machine.

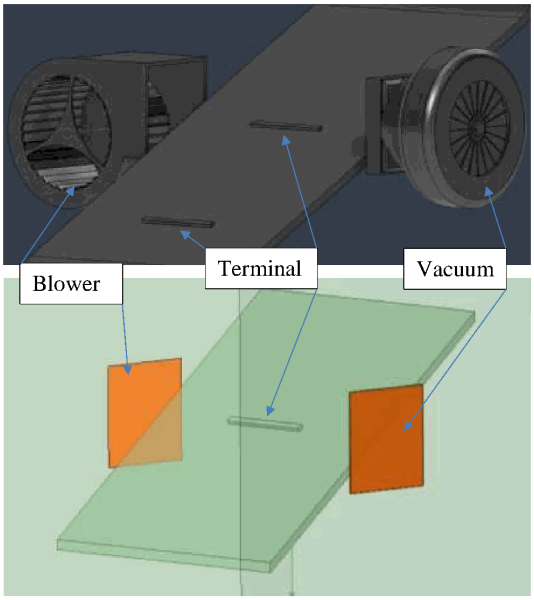


Figure 1. Airflow path of the proposed blower-assisted capture mechanism: CAD layout of the blower, terminal and vacuum on the winding conveyor (top), and the corresponding inlet, terminal and outlet arrangement in the CFD model (bottom).

Several practical constraints shaped the layout. Both units sit beside the conveyor, so they do not interfere with moving parts, material transport or operator access, and they can be retrofitted to existing machines without structural changes. The jet direction was aligned with the machine operation so that it does not disturb product handling. A blower was preferred over compressed air because compressed-air nozzles produce very high local velocities, which tend to scatter particles and disturb nearby components. Mechanical and electrical safety requirements, including guarding, mounting, grounding and cable routing, were also considered in line with ISO 12100. In the CFD model, the blower is represented as a velocity inlet and the vacuum unit as a pressure outlet, which allows the corridor between them to be studied without selecting specific commercial equipment.

3.3 Design Calculations

Opening size. The blower and vacuum openings were sized from the continuity relation Q = AV. For a target flow rate Q = 0.01 m³/s and a design velocity of 4 m/s, the required area is A = 0.0025 m², which corresponds to a 50 mm × 50 mm square opening. With this opening, the velocity range of 3-10 m/s studied later corresponds to flow rates of 0.0075-0.025 m³/s, which is typical of compact industrial blowers.

Terminal stability. The capacitor terminal lies directly in the jet path, so the jet must not move or vibrate it. The terminal has a mass of 0.003 kg, giving a weight of Fg = mg = 0.0294 N. As a conservative criterion, the aerodynamic drag on the terminal was limited to 30% of its weight, that is, Fd ≤ 0.3Fg ≈ 0.009 N. The drag is estimated from

$$F_d = \frac{1}{2} C_d \rho A_t V^2 \qquad (6)$$

where Cd = 1.1 is taken for a bluff rectangular section [13] and At = 6 × 10^{-6} m² is the projected area of the 3 mm × 2 mm terminal cross-section facing the jet. Solving Eq. (6) at the drag limit gives a maximum permissible approach velocity of about 47 m/s. At the highest blower velocity studied, 10 m/s, Eq. (6) gives Fd ≈ 4.0 × 10^{-4} N, about 1.4% of the terminal weight. The 3-10 m/s operating range therefore has a large stability margin, and the velocity can be chosen on the basis of dust transport and flow quality alone.

3.4 Geometry and Mesh

The winding zone was reduced to the parts that shape the local airflow: an air domain, the conveyor and the terminal, as shown in Figure 2. Drive mechanisms, structural frames, electrical components and guards were omitted because their influence on the local flow was judged to be negligible. The domain is a 170 mm × 200 mm × 250 mm box, in which X is the blower-to-vacuum direction, Y is along the conveyor and Z is vertical. The 50 mm × 50 mm blower and vacuum openings are placed on opposite X faces, 170 mm apart. The terminal keeps its actual dimensions of 50 mm × 3 mm × 2 mm.

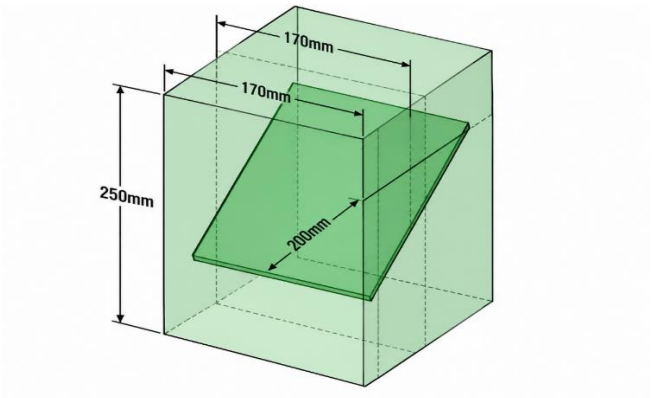


Figure 2. Simplified winding machine model showing the air domain, conveyor, terminal and opposing blower and vacuum openings.

The domain was meshed in ANSYS Meshing with unstructured linear tetrahedra using the Patch Conforming algorithm. Face sizing of 2 mm was applied at the blower

and vacuum openings to resolve the steep velocity gradients there. Inflation layers were not used, because the study targets the bulk flow and particle transport rather than near-wall boundary layers. The geometry and mesh parameters are listed in Table 2. The skewness and orthogonal quality values are within commonly recommended limits for Fluent, namely maximum skewness below 0.95 and minimum orthogonal quality above 0.1 [14].

Table 2. Geometry dimensions and mesh statistics

Item	**Value**
Air domain (X × Y × Z)	170 × 200 × 250 mm
Blower and vacuum openings	50 × 50 mm each, 170 mm apart
Conveyor	150 × 180 × 5 mm
Terminal	50 × 3 × 2 mm
Mesh type	Unstructured tetrahedral, Patch Conforming
Local refinement	2 mm face sizing at inlet and outlet
Nodes / elements	15,642 / 80,979
Skewness (average / maximum)	0.236 / 0.893
Orthogonal quality (average / minimum)	0.763 / 0.107

3.5 Boundary Conditions and Material Properties

The blower opening was defined as a velocity inlet with a uniform normal velocity, which gives direct control over the supplied airflow. The vacuum opening was defined as a pressure outlet at a gauge pressure of -100 Pa, representing the suction of the vacuum unit and producing the pressure difference between the two openings [14]. All other surfaces, including the domain boundaries, conveyor and terminal, were treated as stationary no-slip walls. For the particle phase, the pressure outlet was set to the *escape* condition, so a particle reaching the vacuum opening is counted as captured, while walls used the default *reflect* condition.

Air was modelled with constant properties at standard conditions. The dust was defined as a custom inert particle material, "metallic-dust", whose density of 2700 kg/m³ represents aluminium-based wear debris from the winding foil. Because the particles are inert, no chemical reaction, evaporation or phase change was considered. Table 3 summarises the boundary conditions and material properties.

Table 3. Boundary conditions and material properties

Item	**Setting**
Blower opening	Velocity inlet: 3, 5, 7 or 10 m/s, normal to face
Vacuum opening	Pressure outlet: -100 Pa gauge; DPM escape
Domain walls, conveyor, terminal	Stationary no-slip wall; DPM reflect
Air	$\rho = 1.225$ kg/m³; $\mu = 1.7894 \times 10^{-5}$ kg/m·s
Metallic dust (inert particle)	$\rho p = 2700$ kg/m³
Aluminium (solid parts)	$\rho = 2719$ kg/m³

3.6 Particle Injection and Capture Efficiency

Dust release was modelled with a group injection of 300 particle streams distributed over a small volume around the terminal, midway between the blower and vacuum openings. A distributed source represents generation from a small region of the winding path more realistically than a single release point. All particles were released with zero initial velocity. Their subsequent motion is therefore caused entirely by the airflow, which isolates the effect of each airflow configuration. A single diameter of 5 µm was used, consistent with the fine end of the 3-10 µm range observed for winding dust. Particles were assumed spherical, and collisions, agglomeration and break-up were neglected. Of the 300 streams defined, 277 were tracked by the solver in every case, and this number is used as the basis for the capture statistics. The remaining streams were not tracked due to incomplete trajectory. The injection and DPM settings are listed in Table 4.

Table 4. Particle injection and DPM settings

Parameter	**Value**
Injection type / streams	Group injection, 300 streams defined (277 tracked)
Release zone (X; Y; Z)	83.5-86.5 mm; 105-145 mm; 75-125 mm
Initial particle velocity	0 m/s in all directions
Particle diameter / shape	5 µm (monodisperse) / spherical
Drag law / gravity	Spherical drag / included
Coupling	One-way, steady particle tracking

The capture efficiency η is defined as the fraction of tracked particle streams that leave the domain through the vacuum outlet:

$$\eta = \frac{N_{captured}}{N_{tracked}} \times 100\% \qquad (7)$$

where Ncaptured is the number of streams that reach the vacuum outlet and Ntracked = 277.

3.7 Solution Procedure and Simulation Cases

The airflow was solved with the steady pressure-based solver in ANSYS Fluent [12], [14]. The flow field was first set up with hybrid initialisation, which produces a starting field consistent with the boundary conditions and improves convergence stability. Each run was limited to 1000 iterations, and the scaled residuals of continuity, the three velocity components, k and ε were monitored. In all combined cases, the residuals fell steeply in the first 100 iterations and then levelled off. The velocity and turbulence residuals reached about 10^{-4}-10^{-5}, while the continuity residual levelled off near 10^{-2}. Particle tracking was performed on the converged flow field in each case.

Seven cases were simulated with identical geometry, mesh and particle injection, as listed in Table 5. Cases 1-3 isolate the contribution of each component, and Cases 4-7 vary the blower velocity of the combined system.

Table 5. Simulation cases

Case	Configuration	Blower inlet	Vacuum outlet
1	No system (baseline)	Inactive	Inactive
2	Vacuum only	Inactive	-100 Pa
3	Blower only	Active	Inactive
4	Combined blower-vacuum	3 m/s	-100 Pa
5	Combined blower-vacuum	5 m/s	-100 Pa
6	Combined blower-vacuum	7 m/s	-100 Pa
7	Combined blower-vacuum	10 m/s	-100 Pa

4. Results And Discussion

4.1 Velocity Distribution

Only the combined blower-vacuum cases formed a continuous high-velocity corridor from the blower to the vacuum opening. Figure 3 shows the velocity contours on the conveyor plane and the corresponding velocity vectors for all seven cases, and Table 6 summarises the maximum velocities.

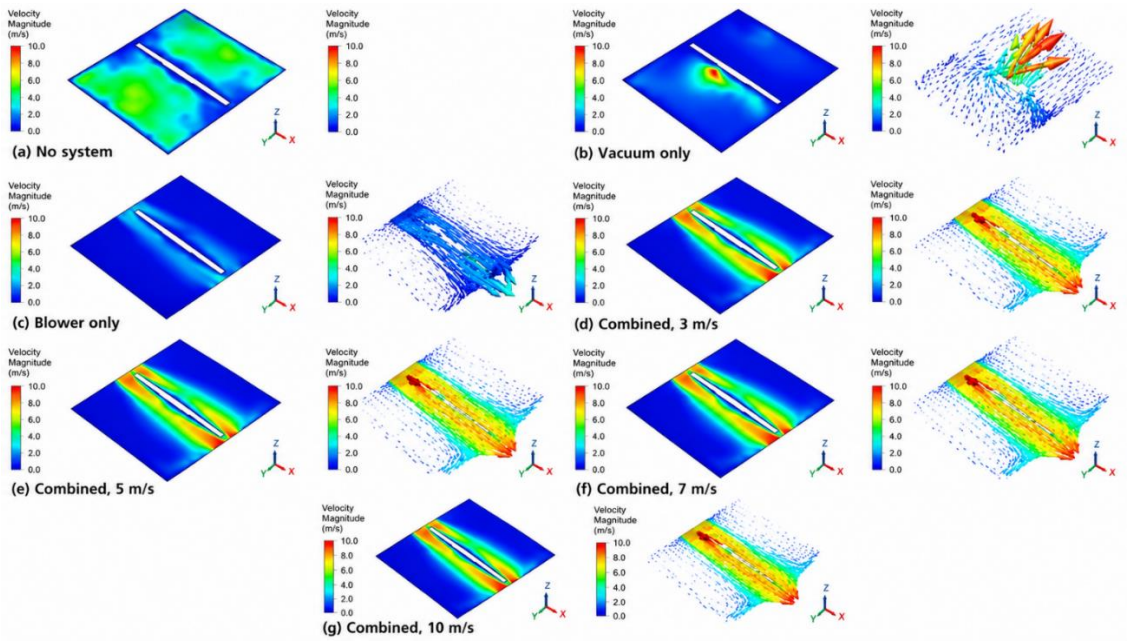


Figure 3. Velocity contours (left of each pair) and velocity vectors (right): (a) no system; (b) vacuum only; (c) blower only; (d)-(g) combined blower-vacuum at 3, 5, 7 and 10 m/s.

In the baseline case (Figure 3a), no boundary drives the flow, and the velocity is essentially zero throughout. Released dust therefore has no transport mechanism other than slow gravitational settling, at about 2 mm/s for 5 µm particles (Section 2.4).

With the vacuum alone (Figure 3b), the flow is confined to a small region in front of the suction opening. The maximum velocity is only 1.32 m/s, and the vectors show that the velocity decays rapidly with distance from the inlet. Away from the opening, the vectors are weak and irregular, and the terminal region lies largely outside the zone of effective suction. This is the short-reach behaviour of exhaust openings described in Section 2.2.

With the blower alone (Figure 3c), a jet enters the domain and moves air across the terminal region. Without suction, however, the jet has no defined sink: it spreads and loses its directional structure before reaching the opposite side, and the vectors show disorganised flow downstream of the terminal.

In the combined cases (Figures 3d-3g), the blower jet and the suction act together to form a well-defined corridor that passes over the terminal and ends at the vacuum opening. The velocity vectors are aligned with the corridor, and the low-velocity regions are confined to the domain edges. The corridor keeps the same shape at every blower velocity, and its intensity increases with the inlet velocity.

Table 6. Maximum velocity and corridor formation for each case

Case	Maximum velocity (m/s)	Ratio to blower velocity	Continuous corridor
No system	≈ 0	-	No
Vacuum only	1.32	-	Partial, near inlet only
Blower only	22.6	-	No
Combined, 3 m/s	3.87	1.29	Yes
Combined, 5 m/s	6.44	1.29	Yes
Combined, 7 m/s	9.00	1.29	Yes
Combined, 10 m/s	12.9	1.29	Yes

The ratio of maximum velocity to blower velocity is 1.29 in all four combined cases. This means the flow pattern is effectively independent of velocity over 3-10 m/s, as expected for fully turbulent flow at Re ≈ 10^4 (Section 2.3). The local acceleration to 1.29 times the inlet velocity is attributed to flow constriction around the terminal and over the conveyor. In practical terms, raising the blower velocity strengthens the corridor without changing its path, so the velocity can be selected for transport performance without redesigning the layout.

4.2 Pressure Distribution

The combined system produced a pressure gradient spanning the whole gap between the blower and the vacuum, and this gradient grew with the square of the blower velocity. Figure 4 shows the static pressure contours, and Table 7 lists the extreme values for each case.

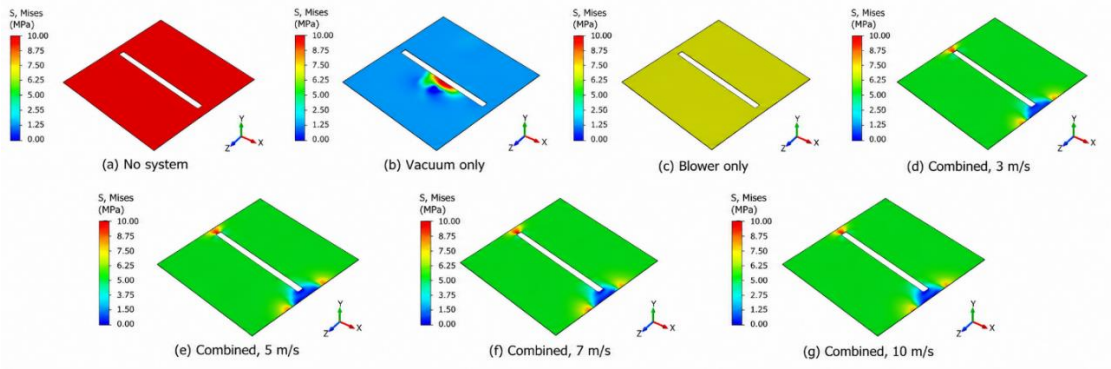


Figure 4. Static pressure contours: (a) no system; (b) vacuum only; (c) blower only; (d)-(g) combined blower-vacuum at 3, 5, 7 and 10 m/s.

In the baseline case (Figure 4a), the pressure field is uniform, so there is no force to move air or dust in any preferred direction. With the vacuum alone (Figure 4b), a low-pressure pocket forms at the suction opening, but the rest of the domain stays at almost the same pressure. The suction therefore affects only the air close to the inlet. With the blower alone (Figure 4c), the pressure rises locally at the jet exit, but without a downstream sink no sustained gradient forms across the domain.

In the combined cases (Figures 4d-4g), the pressure falls steadily from the blower side to the vacuum side, with the largest gradients at the two openings. This gradient is the driving force that holds the corridor seen in Figure 3. The minimum pressure lies slightly below the -100 Pa outlet value because the air accelerates into the outlet.

Table 7. Static pressure extremes and inlet-outlet pressure difference

Case	Max. pressure (Pa)	Min. pressure (Pa)	Δp (Pa)	Δp / (½ρV²)
No system	≈ 0	≈ 0	≈ 0	-
Vacuum only	99.1	-100	199	-
Blower only	228	-279	507	-
Combined, 3 m/s	-91	-101	10	1.81
Combined, 5 m/s	-76	-104	28	1.83
Combined, 7 m/s	-55	-108	53	1.77
Combined, 10 m/s	-8	-117	109	1.78

For the combined cases, the pressure difference Δp across the domain rises from 10 Pa at 3 m/s to 109 Pa at 10 m/s. Normalised by the inlet dynamic pressure ½ρV², it

stays at 1.8 ± 0.03 in all four cases. The pressure loss of the corridor therefore scales with V^2, which is consistent with the constant velocity ratio in Table 6 and confirms that the flow is fully turbulent. In practice, going from 7 m/s to 10 m/s roughly doubles the pressure the blower must supply (53 Pa to 109 Pa) and raises the airflow by 43%. The fan power, which scales with $Q \cdot \Delta p$, increases by a factor of about 2.9.

4.3 Particle Trajectories

The particle tracks in Figure 5 show that only the combined configuration carried the dust from the release zone into the vacuum outlet along organised paths.

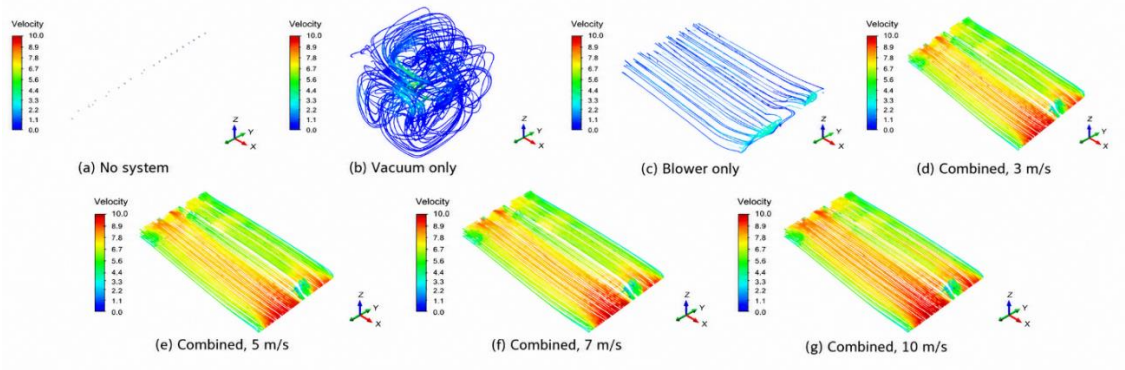


Figure 5. DPM particle tracks coloured by particle velocity: (a) no system; (b) vacuum only; (c) blower only; (d)-(g) combined blower-vacuum at 3, 5, 7 and 10 m/s.

Without any system (Figure 5a), the particles barely move from their release points. This is the current situation, in which dust hangs around the terminal and eventually settles on the product, rollers and sensors.

The vacuum-only case (Figure 5b) is the most revealing. The particles do move, but along closed, looping paths that fill the centre of the domain. The weak suction field sets up recirculation in which particles circulate repeatedly without reaching the outlet. A suction source that only partly reaches the dust zone can therefore keep particles airborne for longer, which in a real machine increases the chance of contaminating a nearby surface.

In the blower-only case (Figure 5c), the particles follow straight, parallel paths in the jet direction. The blower clearly sets the direction of transport. However, with no extraction, the particles are only moved from the terminal region to the opposite side of the machine, not removed.

In all combined cases (Figures 5d-5g), the tracks form a dense, uniform band from the release zone to the vacuum opening, with no recirculating loops. As the blower velocity increases, the tracks shift towards higher particle velocities, so the particles cross the 170 mm gap faster. Their residence time near the terminal is therefore shorter. At 3 m/s, some tracks spread towards the domain edges before turning into the outlet. From 5 m/s upward, the band is tighter and more direct.

The behaviour is consistent with the Stokes number estimate (Stk ≈ 0.01-0.04 over 3-10 m/s). The particles are near-perfect flow tracers, so their paths simply reproduce the airflow pattern. Capture is therefore decided by whether the airflow

connects the release zone to the outlet, which explains the large differences between cases.

4.4 Dust Capture Efficiency

Adding the blower raised the capture efficiency from 27% with the vacuum alone to 100% at every blower velocity tested. Table 8 gives the particle fates computed with Eq. (7).

Table 8. Particle fate and capture efficiency (277 tracked streams per case)

Case	Captured at vacuum outlet	Not captured	Capture efficiency η
No system	0	277	0%
Blower only	0	277	0%
Vacuum only	75	202	27%
Combined, 3 m/s	277	0	100%
Combined, 5 m/s	277	0	100%
Combined, 7 m/s	277	0	100%
Combined, 10 m/s	277	0	100%

The vacuum alone captured only 75 of the 277 streams. The other 202 remained in the recirculating flow of Figure 5b, which is the numerical counterpart of the residual airborne dust observed around the existing vacuum system on site. The blower alone captured nothing because it has no sink. Each component on its own is therefore ineffective, but together they capture every tracked particle. The improvement comes from the interaction between the two: the blower provides the transport path and the vacuum provides the removal.

This trend agrees qualitatively with push-pull studies of larger systems, where adding a push jet raised capture efficiency well above that of exhaust alone [5]. The absolute values here are higher because the source sits directly in the corridor and the domain is small and free of cross-draughts. They should be read as an upper bound for an idealised machine, not as a field prediction (Section 4.6).

4.5 Influence of Blower Velocity and Selection of the Operating Point

A blower velocity of 7 m/s was selected as the operating point, because it gives direct, well-confined transport with a robust margin at moderate power. Because all four combined cases reached $\eta = 100\%$, capture efficiency alone cannot distinguish between them. The selection was therefore based on the quality of transport, the margin against disturbances and the energy cost, summarised in Table 9.

Table 9. Comparison of blower velocities in the combined system

Blower velocity	η	Peak corridor velocity (m/s)	Nominal transit time L/V (ms)	Relative fan power Q·Δp	Track behaviour
3 m/s	100%	3.87	57	0.08	Some spreading towards the edges
5 m/s	100%	6.44	34	0.38	Concentrated band
7 m/s	100%	9.00	24	1.00	Direct, well-confined band
10 m/s	100%	12.9	17	2.94	Direct; stronger turbulence

At 3 m/s, the corridor is complete but weak. Some tracks spread before turning into the outlet, so the margin against disturbances not included in the model is small. Such disturbances include roller-induced air currents, operator movement and room ventilation. As a reference point, recommended capture velocities for local exhaust range from about 0.5 m/s for dust released into quiet air to about 2.5 m/s for actively generated dust. A corridor velocity of only 3-4 m/s leaves little reserve above the upper end of that range.

At 5 m/s, the tracks are noticeably more concentrated. At 7 m/s, the corridor is strong and uniform, the tracks run directly to the outlet, and the transit time across the terminal zone falls to about 24 ms.

Raising the velocity further to 10 m/s brings no gain in capture, and the transit time shortens only slightly, from 24 to 17 ms. In exchange, the fan power rises by a factor of about 2.9 relative to 7 m/s, and the flow becomes more turbulent. Stronger turbulence increases the risk of re-entraining settled dust and disturbing light foil or nearby components. The terminal itself remains stable at all velocities (Section 3.3).

The 7 m/s case therefore offers the best balance: complete and direct transport with a healthy margin, at about one-third of the power needed at 10 m/s.

4.6 Limitations

The results should be read as a numerical feasibility study, for the following reasons.

First, the geometry is simplified. Rotating rollers, moving foil and surrounding equipment were omitted, so roller-induced air currents and cross-draughts, which would compete with the corridor, are not represented.

Second, the simulations are steady-state with one-way coupled, monodisperse 5 µm spherical particles. One-way coupling is appropriate for the very dilute dust loadings involved. Transient dust release, irregular particle shapes, a size distribution and stochastic turbulent dispersion, for example with a discrete random walk model, were not modelled, and non-spherical drag corrections were not applied. These factors would make some particle paths more scattered and would likely lower the 100% efficiencies.

Third, a mesh-independence study was not performed, no inflation layers were used near the walls, and the continuity residual levelled off at a relatively high value. A grid convergence study on coarse, medium and fine meshes and a check of the outlet mass balance would strengthen confidence in the predicted flow field.

Finally, the predictions have not been validated experimentally. Measurements of velocity at the corridor centreline and of dust concentration near the terminal, for example with an optical particle sensor, are needed before the results are used for industrial design.

5. Conclusion

A blower-assisted vacuum dust capture mechanism for capacitor winding machines was designed and evaluated using CFD with the realizable k-ε model and one-way coupled DPM particle tracking. Seven configurations were compared under identical conditions, and the main findings are as follows.

1. Neither component works well alone. The vacuum alone captured only 27% of the tracked particle streams, because its velocity field decayed rapidly and created recirculation that kept particles airborne. The blower alone captured none, because it moved particles across the domain without removing them.
2. Combining the two units formed a continuous airflow corridor from the blower to the vacuum, driven by a pressure gradient across the whole gap. This corridor transported all 277 tracked particle streams to the outlet at every blower velocity from 3 to 10 m/s.
3. Over this range, the flow was self-similar. The peak velocity remained 1.29 times the blower velocity, and the pressure difference remained 1.8 times the inlet dynamic pressure. Raising the blower velocity therefore strengthens the corridor without changing its path.
4. A blower velocity of 7 m/s is recommended. It gives direct, well-confined particle transport with a good margin against disturbances. In contrast, 10 m/s adds no capture benefit, needs about 2.9 times the fan power and increases turbulence.
5. Drag on the capacitor terminal at 10 m/s is only about 1.4% of its weight, far below the stability limit that corresponds to about 47 m/s. The jet therefore poses no risk to terminal stability over the studied range.

These results show that guiding the airflow towards an existing suction point is more effective than relying on suction alone. The mechanism needs only a compact blower opposite the existing vacuum inlet, so it can be retrofitted to winding machines without structural changes. In practice, this could reduce dust deposition on terminals and false rejections at electrical testing.

Future work should first validate the model on a physical prototype, using velocity measurements and particle counts near the terminal. The model should then be extended to include rotating rollers, moving foil and transient operation. Polydisperse, non-spherical particles with stochastic turbulent dispersion should also be considered. Finally, the realizable k-ε results should be cross-checked against an alternative model such as SST k-ω.

Acknowledgement
The authors thank the Faculty of Electrical Technology and Engineering, Universiti Teknikal Malaysia Melaka (UTeM), for providing the facilities and software used in this study. They also thank the industrial partner for granting access to its winding machine operations.

References

[1] Qian, J., Wang, J., Liu, H., and Xu, H., 2020, "CFD Modeling of Ventilation and Dust Flow Behavior in Polishing and the Design of an Innovative Wet Dust Removal System," International Journal of Environmental Research and Public Health, 17(16), 6006.

[2] Yao, H., Qiu, S., Lv, Y., Wei, S., Li, A., Long, Z., Wu, W., & Shen, X., 2023, "Indoor Particulate Matter Transfer in CNC Machining Workshop and The Influence of Ventilation Strategies-A Case Study," Sustainability, 15(7), 6227.

[3] Jian, W., 2012, "Research on damage control of dust pollution in machine processing," Science & Technology Vision.

[4] Anlimah, F., Gopaldasani, V., MacPhail, C., & Davies, B., 2023, "A systematic review of the effectiveness of dust control measures adopted to reduce workplace exposure," Environmental Science and Pollution Research, 30(19), 54407–54428.

[5] Kulmala, I., Hynynen, P., Welling, I., and Säämänen, A., 2007, "Local Ventilation Solution for Large, Warm Emission Sources," Annals of Occupational Hygiene, 51(1), pp. 35-43.

[6] Hong, Y., Huang, B., & Zhu, D. Z., 2025, "Hydraulic optimization of a stormwater pumping station by physical and computational fluid dynamics modeling," Engineering Applications of Computational Fluid Mechanics, 19(1).

[7] Ayo, S. A., & Mohd-Ghazali, N., 2024, "Numerical Simulation of the Interference Effects to Outdoor Air Flow and Ventilation around Adjacent Building Arrays," QIR (Kyushu University Institutional Repository), 11(1), 402–416.

[8] Fan, L., & Liu, S., 2021, "Respirable nano-particulate generations and their pathogenesis in mining workplaces: a review," International Journal of Coal Science & Technology, 8(2), 179-198.

[9] Gottschalk, J., & Stellmer, S., 2024, "Demystifying dust contamination in quantum optics labs: measurements and recommendations," In arXiv, Cornell University.

[10] Meng, Q., Wang, F., Li, Q., Wang, X., Lin, C., and Wang, X., 2022, "Optimization Research Based on Local Exhaust of Oil Mist Particles in Cutting Machine Tool," E3S Web of Conferences, 356, 05082. https://doi.org/10.1051/e3sconf/202235605082

[11] Versteeg, H. K., and Malalasekera, W., 2007, "An Introduction to Computational Fluid Dynamics: The Finite Volume Method," 2nd ed., Pearson Education, Harlow.

[12] ANSYS Inc., 2021, ANSYS Fluent Theory Guide, Release 2021 R1, ANSYS Inc., Canonsburg, PA.

[13] Çengel, Y. A., and Cimbala, J. M., 2018, Fluid Mechanics: Fundamentals and Applications, 4th ed., McGraw-Hill Education, New York.

[14] ANSYS Inc., 2022, ANSYS Fluent User's Guide, Release 2022 R1, ANSYS Inc., Canonsburg, PA.